

Bloch surface waves-controlled fluorescence emission: coupling into nanometer-sized polymeric waveguides

Original

Bloch surface waves-controlled fluorescence emission: coupling into nanometer-sized polymeric waveguides / Ballarini, Mirko; Frascella, Francesca; Enrico, Emanuele; Mandracci, Pietro; De Leo, N.; Michelotti, F.; Giorgis, Fabrizio; Descrovi, Emiliano. - In: APPLIED PHYSICS LETTERS. - ISSN 0003-6951. - 100:(63305)(2012). [10.1063/1.3684272]

Availability:

This version is available at: 11583/2495800 since:

Publisher:

AIP

Published

DOI:10.1063/1.3684272

Terms of use:

This article is made available under terms and conditions as specified in the corresponding bibliographic description in the repository

Publisher copyright

(Article begins on next page)

Bloch surface waves-controlled fluorescence emission: Coupling into nanometer-sized polymeric waveguides

Mirko Ballarini, Francesca Frascella, Emanuele Enrico, Pietro Mandracci, Natascia De Leo et al.

Citation: *Appl. Phys. Lett.* **100**, 063305 (2012); doi: 10.1063/1.3684272

View online: <http://dx.doi.org/10.1063/1.3684272>

View Table of Contents: <http://apl.aip.org/resource/1/APPLAB/v100/i6>

Published by the [American Institute of Physics](#).

Related Articles

A realistic design of three-dimensional full cloak at terahertz frequencies

Appl. Phys. Lett. **101**, 031910 (2012)

Plasma-accelerated flyer-plates for equation of state studies

Rev. Sci. Instrum. **83**, 073504 (2012)

Operational lifetime improvement of poly(9,9-dioctylfluorene) active waveguides by thermal lamination

Appl. Phys. Lett. **101**, 013303 (2012)

Operational lifetime improvement of poly(9,9-dioctylfluorene) active waveguides by thermal lamination

APL: Org. Electron. Photonics **5**, 143 (2012)

Efficient optical gain media comprising binary blends of poly(3-hexylthiophene) and poly(9,9-dioctylfluorene-co-benzothiadiazole)

J. Appl. Phys. **111**, 123107 (2012)

Additional information on *Appl. Phys. Lett.*

Journal Homepage: <http://apl.aip.org/>

Journal Information: http://apl.aip.org/about/about_the_journal

Top downloads: http://apl.aip.org/features/most_downloaded

Information for Authors: <http://apl.aip.org/authors>

ADVERTISEMENT



AIP Advances

Special Topic Section:
PHYSICS OF CANCER

Why cancer? Why physics? [View Articles Now](#)

Bloch surface waves-controlled fluorescence emission: Coupling into nanometer-sized polymeric waveguides

Mirko Ballarini,¹ Francesca Frascella,¹ Emanuele Enrico,² Pietro Mandracci,¹ Natascia De Leo,² Francesco Michelotti,³ Fabrizio Giorgis,¹ and Emiliano Descrovi^{1,a)}

¹Department of Applied Science and Technology, Politecnico di Torino, c.so Duca degli Abruzzi 24, 10129 Torino, Italy

²National Institute of Metrological Research, strada delle Cacce 91, 10135 Torino, Italy

³Department of Basic and Applied Sciences for Engineering, SAPIENZA Università di Roma, via A. Scarpa 16, 00161 Roma, Italy

(Received 12 October 2011; accepted 20 January 2012; published online 10 February 2012)

The lateral confinement of Bloch surface waves on a patterned multilayer is investigated by means of leakage radiation microscopy (LRM). Arrays of nanometric polymeric waveguides are fabricated on a proper silicon-nitride/silicon-oxide multilayer grown on a standard glass coverslip. By exploiting the functional properties of the polymer, fluorescent proteins are grafted onto the waveguides. A fluorescence LRM analysis of both the direct and the Fourier image plane reveals that a substantial amount of emitted radiation couples into a guided mode and then propagates into the nanometric waveguide. The observations of the mode are supported by numerical simulations. © 2012 American Institute of Physics. [doi:10.1063/1.3684272]

Bloch surface waves (BSWs) are either TE- or TM-polarized electromagnetic waves that can be coupled at the surface of proper truncated periodical structures such as multilayers or one-dimensional photonic crystals (1DPC).¹ In analogy to dielectric-loaded waveguides for surface plasmon polaritons (SPPs) on smooth metallic films,² BSWs can be confined to some extent on ultra-thin relieves of micrometric lateral dimension.^{3,4} As explained elsewhere,⁵ this effect is due to a combined role of the remarkably narrow energy/momentum BSW resonance and the redshift experienced by the BSW resonance upon a slight surface perturbation, such as the deposition of a small amount of organic adlayer. Opposite to SPPs in dielectric-loaded waveguides, BSWs on nanometric relieves still preserve their inherent surface mode features and are, therefore, particularly suited for sensing applications.

In a recent work, a BSW-controlled fluorescence emission of dye-labelled proteins on a planar dielectric 1DPC has been demonstrated,⁶ showing a remarkable emission enhancement and a narrow beaming effect. Here, we take the investigation of BSW-controlled fluorescence a step further and demonstrate the significant coupling and guidance effect of the emitted radiation from fluorescent labeled proteins A (PtA) grafted on ultra-thin, polymeric channel waveguides on a proper dielectric 1DPC. Experimental observations are performed by means of a custom setup based on leakage radiation microscopy (LRM),⁷ schematically presented in Fig. 1(a). This wide-field imaging technique is widely used for investigating evanescent electromagnetic modes (mainly surface plasmons) in interaction with a number of nanostructures and/or emitters including, e.g., plasmonic waveguides,⁸ plasmonic emitting nano-wires,⁹ gratings¹⁰ and nanoparticle arrays,¹¹ or plasmons interfering with one another.¹²

The 1DPC consists of a stack of 8 periods of paired high (H) and low (L) refractive index layers of amorphous silicon-based alloys ($\text{Si}_x\text{N}_{1-x}$, $n_H = 1.99$ and SiO_2 , $n_L = 1.48$ at $\lambda = 532$ nm) with thickness $d_H = 60$ nm and $d_L = 160$ nm, respectively, deposited on a thin glass coverslip by plasma enhanced chemical vapor deposition (PECVD). On such a 1DPC, TE-polarized BSWs are supported. Nanometric ridges are fabricated by means of electron beam lithography (EBL) followed by a plasma-polymerized acrylic acid (PPAAc) deposition (30 nm thickness) and a liftoff

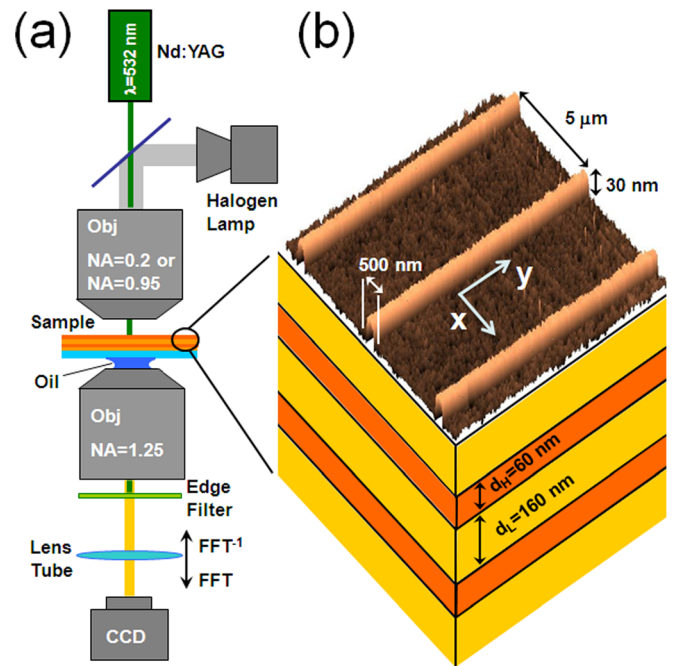


FIG. 1. (Color online) (a) Sketch of the leakage radiation microscope: by moving the tube lens along the optical axis, either the FFT or FFT^{-1} plane can be imaged and (b) comprehensive representation of the dielectric 1DPC (drawing) and the corresponding patterned surface (AFM measurement on top).

^{a)}Author to whom correspondence should be addressed. Electronic mail: emiliano.descrovi@polito.it.

procedure in acetone. AlexaFluor 546(AF546)-labelled PtA is finally grafted on the polymer and rinsed (see supplementary material for fabrication details).¹⁶

A sketch of the 1DPC, together with an AFM topographic map of the patterned surface, is presented in Fig. 1(b). As shown in Fig. 1(a), the sample is illuminated from the air side by means of a laser source emitting at 532.0 nm focused by either a NA = 0.2 or a NA = 0.95 objective. The fluorescent PtA grafted on the polymeric waveguides are excited, and part of the emitted fluorescence couples to the BSW modes sustained by the 1DPC. As the 1DPC is truncated, these modes are leaky into the substrate and a portion of the emitted fluorescence propagating in the glass can be collected from the bottom side of the multilayer by means of an immersion-oil objective (NA = 1.25) and then imaged onto a CCD. The direct (FFT^{-1}) as well as the reciprocal image (Fourier or FFT plane) of the light distribution on the sample surface can be obtained by simple adjustment of a sliding tube lens in front of the CCD camera. An edge filter placed beneath the collection objective filters out the leaking laser radiation used for the excitation.

As a first experiment, we considered a flat 1DPC homogeneously coated with fluorescent PtA on an additional PPAA layer 30 nm thick. We previously showed that the fluorescence leaking into the glass substrate is preferentially coupled to BSWs sustained by the 1DPC.⁶

When the BSW-coupled fluorescence is FFT-imaged (focusing objective: NA = 0.2), the collected fluorescence is mainly contained in the annular region defined by $1 < k_T/k_0 < 1.25$, where k_0 is the wavevector in vacuum and $k_T = (k_x^2 + k_y^2)^{1/2}$ is the in-plane component of the wavevector in the object plane (Fig. 2(a)). This annular region corresponds to propagation directions of light running beyond the glass/air light line ($k_T/k_0 = 1$): therefore, it is the portion of fluorescence trapped in the substrate due to total internal reflection.

In addition, one also can see that a significant amount of fluorescence is confined in a narrow wavevector range, due to strong coupling to the BSW mode. This pattern results from the incoherent sum of a set of contiguous, concentric circles whose radii correspond to the in-plane (xy-plane)

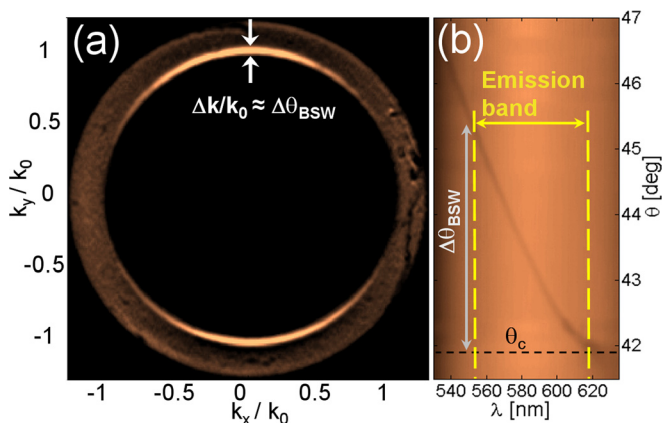


FIG. 2. (Color online) (a) FFT plane image of x-polarized BSW-coupled fluorescence coupled onto a homogeneous sample and (b) Angle-resolved reflectance map of 1DPC as measured by means of a prism-based goniometric setup.⁶

wavevector components of fluorescent BSWs at different emission wavelengths. Contiguous circles result in a narrow ring of azimuthally polarized light¹³ in the imaged plane. Note that for SPPs, the FFT pattern follows a radially polarized distribution.¹⁴ If a x-oriented polarizer is inserted after the collection objective, the resulting pattern is distributed as y-aligned bright, narrow arcs corresponding to TE-polarized BSWs propagating with large divergence in the y-direction on the 1DPC top surface (Fig. 2(a)).

The width of each of the bright arcs, $\Delta k/k_0$, corresponds to an angular range $\Delta \theta_{\text{BSW}}$ in which all polychromatic BSW-coupled fluorescence components leak out of the glass substrate. After proper sizing of the FFT image presented in Fig. 2(a), such an angular range $\Delta \theta_{\text{BSW}}$ is estimated to be $\approx 3.6^\circ$. This value is in good agreement with the estimate of the angular coupling region of BSWs related to the emission spectrum of the dye grafted on the 1DPC surface. In Fig. 2(b), a prism-based measurement of the angularly resolved reflectance map of the 1DPC is presented (see supplementary material for experimental details),¹⁶ in which the BSW dispersion curve appears as a low reflectivity (dark) narrow region. By projecting onto the θ -axis, the intersection points of the AlexaFluor 546 emission band with the measured BSW dispersion, we find that $\Delta \theta_{\text{BSW}} \approx 3.5^\circ$. This demonstrates that the width of the bright arcs in the FFT image of Fig. 2(a) is due to the fluorescence broadband emission. In addition, from Fig. 2(b), we observe that the BSW dispersion is very close to the critical angle θ_c (and it actually extends even beyond the critical angle—indicated by a dotted line in the figure—where it leaks in air). For this reason, the two arcs in the FFT image of Fig. 2(a) are practically lower-limited by $k_T/k_0 = 1$.

Turning now to a patterned sample, a set of waveguides is simultaneously illuminated by means of a low NA objective (NA = 0.2), used as a collimator (the incoming beam is focused on the back focal plane of the objective). In this way, a rather homogeneous illumination spot of roughly $50 \mu\text{m} \times 50 \mu\text{m}$ is obtained. In Fig. 3(a), the fluorescence LRM-image recorded in the FFT plane from a set of 30 nm thick, 500 nm wide waveguides is shown.

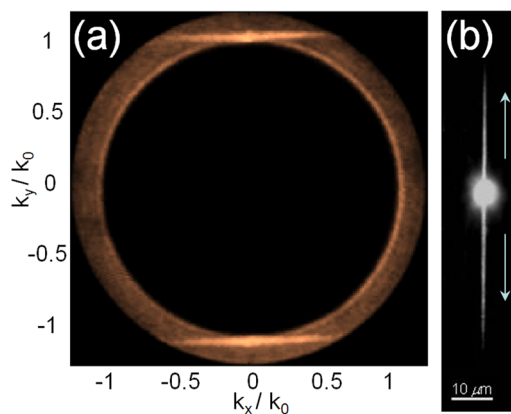


FIG. 3. (Color online) (a) FFT plane image of x-polarized BSW-coupled fluorescence on a patterned sample. The fluorescence coupling in the fundamental guided mode is visible as a sharp horizontal line beyond the air light line (dark circle) and (b) FFT^{-1} plane image of a single waveguide with propagating fluorescent guided BSW arranged in the fundamental mode.

Similarly to dielectric loaded plasmonic waveguides,¹⁵ the bright horizontal lines are the signature of the waveguide modes leaking into the photonic structure, thus demonstrating the coupling of the fluorescence and the BSW modes. The momentum shift induced by the presence of the polymeric waveguide thickness is small, but large enough to provide a preferential coupling of the emitted radiation into the (fundamental) mode sustained by the structure. In order to have a clear evidence of such a coupling, a single waveguide is illuminated by means of a high NA focusing objective (NA=0.95). Fig. 3(b) shows the waveguide BSW-coupled fluorescence as imaged in the FFT^{-1} (direct) plane. A rough estimation of the longitudinal extension of such a guided mode is found to be about $40\ \mu\text{m}$. However, as well known in the field, the decay length obtained analyzing data close to the region of direct illumination tends to be underestimated, due to the presence all those k -contributions that do not match perfectly to the propagation constant of the mode. Therefore, we expect the real value to be larger.

The propagation of the guided BSW mode supported by the 1DPC and polymer strip system was simulated by means of a beam propagation method. In Fig. 4, we show the xz -plane distribution of the square modulus of the guided BSW electric field $|E(x,z)|^2$ calculated at $\lambda=575\ \text{nm}$, where the AF546 fluorescence is peaked. A cross sectional profile of $|E(x,z_0)|^2$ is also shown at a height $z_0=10\ \text{nm}$ above the top of the polymer ridge. Despite the very low-aspect ratio, the structure confines the radiation into a mode with a lateral spread comparable to the size of the polymeric ridge (approximately $600\ \text{nm}$). In Fig. 4, it is also shown that the guided mode slightly leaks into the substrate due to the finite number of periods of the 1DPC. The fact that the width is close to cutoff for transverse confinement is responsible for the two small lobes protruding for the side of the ridge and

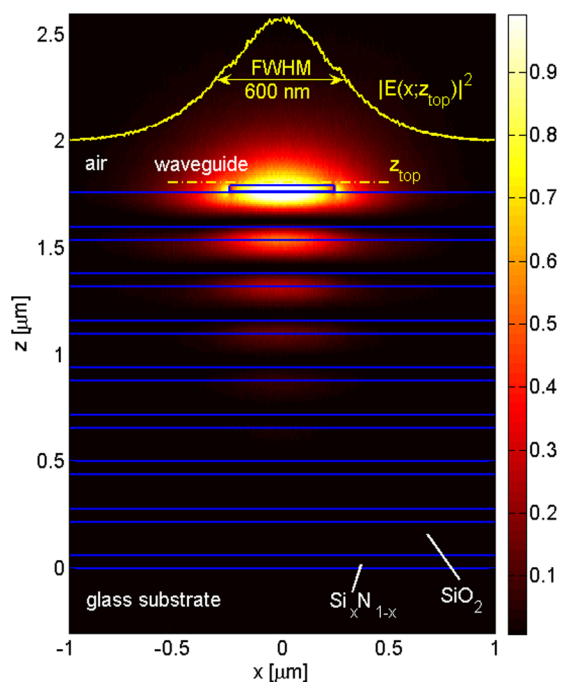


FIG. 4. (Color online) xz -plane distribution of normalized $|E(x,z)|^2$ associated to the fundamental guided mode of a single waveguide on 1DPC.

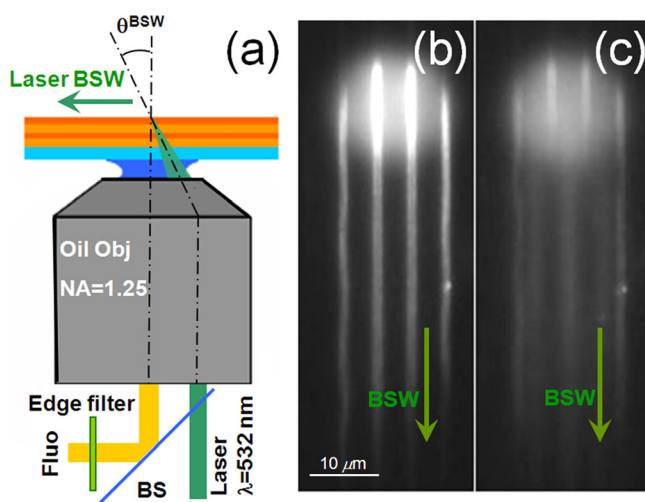


FIG. 5. (Color online) (a) Schematics of the setup used for direct BSW laser coupling. FFT^{-1} fluorescence images of the laser coupled to the BSWs sustained by the waveguides (b) and by the 1DPC bare surface (c).

for scattering losses. Nevertheless, for such a leaky mode, calculations predict a propagation length as large as $150\ \mu\text{m}$ with an absorption of $\text{Im}\{n\} = 2 \times 10^{-4}$, for both silicon nitride and silicon oxide layers.

As a final issue, we speculate about the origin of the diffused fluorescence propagating in the substrate with $1 < k_T/k_0 < 1.25$, uncoupled to BSW modes. That detected intensity might arise from light laterally leaking out of the nanometric waveguides because of refraction⁴ or from fluorescence coming from the outside of the waveguide (some amount of labeled PtA may nevertheless bind onto the bare 1DPC surface). Additional observations suggest that a combination of the above mentioned two effects takes place. In fact, when fluorescent dyes on the waveguides are preferentially excited by a direct coupling of the illuminating laser beam to the guided BSW (by using the oil immersion objective as a prism and displacing the collimated incident beam slightly off-axis with respect to the optical axis) as illustrated in Fig. 5(a), then the image in Fig. 5(b) is obtained, showing a high contrast level for regions inside/outside the waveguides, with still some amount of background fluorescence. Instead, when the illuminating laser beam is steered in such a way that the BSW outside the waveguides is coupled (in Ref. 3, such an angular-selective coupling has been demonstrated on a prism-based setup), the resulting image contrast is lowered (Fig. 5(c)), meaning that a residual amount of fluorescent PtA is nevertheless grafted on the bare 1DPC regions and directly excited by the laser BSW.

In conclusion, we have demonstrated that BSW-controlled fluorescence can be coupled and laterally confined on almost flat guiding structures with nanometer-sized polymeric relieves implementing photonic and chemical functionality at the same time. We acknowledge that this finding may be mostly useful for sensing applications but it could be applied also to other domains such as gain-assisted surface waves on doped structured media.¹⁵

The authors acknowledge the collaboration with Nano-Facility Piemonte, INRiM, a laboratory supported by Compagnia di San Paolo. This work is funded by the Piedmont

Regional Project CIPE 2008 “PHotonic biOsensors for Early caNcer diagnostICS (PHOENICS).”

- ¹P. Yeh, A. Yariv, and A. Y. Cho, *Appl. Phys. Lett.* **32**, 104 (1978).
- ²T. Goto, Y. Katagiri, H. Fukuda, H. Shinojima, Y. Nakano, I. Kobayashi, and Y. Mitsuoka, *Appl. Phys. Lett.* **84**, 852 (2004).
- ³E. Descrovi, T. Sfez, M. Quaglio, D. Brunazzo, L. Dominici, F. Michelotti, H. P. Herzig, O. J. F. Martin, and F. Giorgis, *Nano Lett.* **10**, 2087 (2010).
- ⁴T. Sfez, E. Descrovi, L. Yu, M. Quaglio, L. Dominici, W. Nakagawa, F. Michelotti, F. Giorgis, and H. P. Herzig, *Appl. Phys. Lett.* **96**, 151101 (2010).
- ⁵T. Sfez, E. Descrovi, L. Yu, D. Brunazzo, M. Quaglio, L. Dominici, W. Nakagawa, F. Michelotti, F. Giorgis, O. J. F. Martin, and H. P. Herzig, *J. Opt. Soc. Am B* **27**, 1617 (2010).
- ⁶M. Ballarini, F. Frascella, F. Michelotti, G. Digregorio, P. Rivolo, V. Paeder, F. Giorgis, and E. Descrovi, *Appl. Phys. Lett.* **99**, 043302 (2011).
- ⁷L. Novotny and B. Hecht, *Principles of Nano-Optics* (Cambridge University Press, New York, 2006).
- ⁸B. Steinberger, A. Hohenau, H. Ditlbacher, A. L. Stepanov, A. Drezet, F. R. Aussenegg, A. Leitner, and J. R. Krenn, *Appl. Phys. Lett.* **88**, 094104 (2006).
- ⁹T. Shegai, V. D. Miljkovic, K. Bao, H. Xu, P. Nordlander, P. Johansson, and M. Kall, *Nano Lett.* **11**, 706 (2011).
- ¹⁰S. P. Frisbie, C. Chesnutt, M. E. Holtz, A. Krishnan, L. Grave de Peralta, and A. A. Bernussi, *IEEE Photon. J.* **1**, 153 (2009).
- ¹¹I. P. Radko, S. I. Bozhevolnyi, A. B. Evlyukhin, and A. Boltasseva, *Opt. Express* **15**, 6576 (2007).
- ¹²L. Grave de Peralta, *J. Opt. Soc. Am B* **27**, 1513 (2010).
- ¹³T. Grosjean, M. Suarez, and A. Sabac, *Appl. Phys. Lett.* **93**, 231106 (2008).
- ¹⁴A. Drezet, A. Hohenau, D. Koller, A. Stepanov, H. Ditlbacher, B. Steinberger, F. R. Aussenegg, A. Leitner, and J. R. Krenn, *Mater. Sci. Eng. B* **149**, 220 (2008).
- ¹⁵J. Grandidier, G. Colas des Francs, S. Massenot, A. Bouhelier, J.-C. Weeber, L. Markey, and A. Dereux, *J. Microsc.* **239**, 167 (2010).
- ¹⁶See supplementary material at <http://dx.doi.org/10.1063/1.3684272> for fabrication details and experimental details.